

# Planetary embryos and planetesimals residing in thin debris discs

Alice C. Quillen,<sup>1</sup>\*† Alessandro Morbidelli<sup>2</sup>† and Alex Moore<sup>1</sup>†

<sup>1</sup>*Department of Physics and Astronomy, University of Rochester, Rochester, NY 14627, USA*

<sup>2</sup>*Observatoire de la Côte d’Azur, BP 4229, 06304 Nice Cedex 4, France*

Accepted 2007 July 6. Received 2007 July 5; in original form 2007 May 9

## ABSTRACT

We consider constraints on the planetesimal population residing in the discs of AU Microscopii (AU Mic),  $\beta$  Pictoris ( $\beta$  Pic) and Fomalhaut taking into account their observed thicknesses and normal disc opacities. We estimate that bodies of radius 5, 180 and 70 km are responsible for initiating the collisional cascade accounting for the dust production for AU Mic,  $\beta$  Pic and Fomalhaut’s discs, respectively, at break radii from the star where their surface brightness profiles change slope. Larger bodies, of radius 1000 km and with surface density of the order of  $0.01 \text{ g cm}^{-2}$ , are required to explain the thickness of these discs assuming that they are heated by gravitational stirring. A comparison between the densities of the two sizes suggests the size distribution in the largest bodies is flatter than that observed in the Kuiper belt. AU Mic’s disc requires the shallowest size distribution for bodies with radius greater than 10 km suggesting that the disc contains planetary embryos experiencing a stage of runaway growth.

**Key words:** stars: individual: AU Microscopii – stars: individual: Beta Pictoris – stars: individual: Fomalhaut – planetary systems: formation – planetary systems: protoplanetary discs.

## 1 INTRODUCTION

Recent visible band images taken with the Advanced Camera for Surveys on the *Hubble Space Telescope* well resolve the vertical scaleheight of two edge on debris discs, the 12-Myr-old (Barrado y Navascues et al. 1999; Zuckerman et al. 2001) dusty circumstellar discs of the M1Ve star AU Microscopii (AU Mic) and the A5V star  $\beta$  Pictoris ( $\beta$  Pic) (Krist et al. 2005; Golimowski et al. 2006). Also resolved is the inner edge of Fomalhaut’s eccentric ring, also allowing a measurement of the disc scaleheight (Kalas, Graham & Clampin 2005). The vertical scaleheight,  $H$ , is related to the inclination dispersion of dust particles and so allows an estimate of the velocity dispersion of the smallest particles. The velocity dispersion of planetesimals sets the energy of interparticle collisions and so affects a calculation of the dust production rate through a collisional cascade (e.g. Kenyon 2002; Wyatt & Dent 2002; Dominik & Decin 2003; Wyatt et al. 2007). The velocity dispersion is also sensitive to the presence of larger bodies in the disc as gravitational scattering or stirring causes an increase in the velocity dispersion with time (e.g. Stewart & Ida 2000; Kenyon & Bromley 2001). Here, by combining observations of observed vertical thickness with estimates for the dust production and gravitational stirring rates, we will place constraints on the underlying planetesimal population in these discs. Because of the difficulty in resolving vertical structure, previous cascade calculations have not used a velocity dispersion

consistent with that estimated for these discs or estimated the role of gravitational stirring.

## 2 SCALING ACROSS THE COLLISIONAL CASCADE

We consider three discs with resolved vertical scaleheights. The properties of these three systems along with the quantities we estimate from them are listed in Table 1. For Fomalhaut, we list properties in the ring edge. For AU Mic and  $\beta$  Pic, we list properties at the radius,  $r$ , from the star where there is break in the surface brightness profile. Models taking into account dust collisions and radiation pressure predict that interior to the break radius the disc is likely to contain dust producing planetesimals whereas exterior to this radius, the dust distribution could be dominated by small particles on highly eccentric orbits that were generated from the disc interior (Augereau & Beust 2006; Strubbe & Chiang 2006).

One of the observed quantities listed in Table 1 is the optical depth,  $\bar{\tau}(\lambda)$ , at wavelength,  $\lambda$ , normal to the disc plane. Because the absorption or the emissivity coefficient of a dust grain with radius  $a$  is reduced for  $\lambda > a$ , and there are more dust grains with smaller radii, we expect the optical depth to be related to the number density of particles of radius  $a \sim \lambda$  (e.g. see discussion in section 4 by Wyatt & Dent 2002). As we only detect the dust particles in scattered light or in thermal emission, we use scaling arguments to estimate the number of larger bodies residing in the disc.

Another observed quantity is the disc thickness that we describe in terms of a scaleheight  $H$  that here is a half-width. The disc aspect ratio is the scaleheight divided by radius,  $h \equiv H/r$ . A population of low-inclination orbits has  $\langle z^2 \rangle \approx \frac{r^2 \langle i^2 \rangle}{2}$ , so  $\bar{i} \sim \sqrt{2}h$ . Here,

\*Visitor, Observatoire de la Côte d’Azur.

†E-mail: aquillen@pas.rochester.edu (ACQ); morby@obs-nice.fr (AM); amoore6@mail.rochester.edu (AM)

**Table 1.** Debris discs with measured thicknesses.

Stellar and disc properties				
Row		AU Mic	$\beta$ Pic	Fomalhaut
1	$M_*(M_\odot)$	0.59	1.75	2.0
2	Age (Myr)	12	12	200
3	$r(\text{au})$	30	100	133
4	$h$	0.019	0.05	0.013
5	$\bar{\tau}(\lambda, r)$	$3 \times 10^{-3}$	$5 \times 10^{-3}$	$1.6 \times 10^{-3}$
6	$\lambda$ ( $\mu\text{m}$ )	1	10	24
Estimated planetesimal properties				
7	$a_{\text{top}}(\text{km})$	4	180	68
8	$\Sigma(a_{\text{top}})$ ( $\text{g cm}^{-2}$ )	0.000 05	0.005	0.002
9	$\Sigma m(a_{\text{top}})$ ( $\text{g}^2 \text{cm}^{-2}$ )	$10^{14.5}$	$10^{21.0}$	$10^{18.8}$
10	$\Sigma m(a_s)$ ( $\text{g}^2 \text{cm}^{-2}$ )	$10^{24.1}$	$10^{26.2}$	$10^{22.7}$

By Row. (1) References for the stellar masses: Houdebine & Doyle (1994), Crifo et al. (1997) and Song et al. (2001), respectively. (2) References for the ages: Barrado y Navascues et al. (1999), Barrado y Navascues (1998). (3) The radii are chosen to be where there is a break in the surface brightness profile as described by Krist et al. (2005), Golimowski et al. (2006) and Kalas et al. (2005), respectively. (4) The aspect ratio  $h = H/r$  for  $H$  the half-width half-max of the disc at radius  $r$ . Aspect ratios are taken from the same references as the break radii listed in Row 3. (5, 6) The normal disc opacity  $\bar{\tau}$  at wavelength  $\lambda$  is given. References for normal disc opacities: the normal disc opacity for AU Mic is estimated for  $1 \mu\text{m}$  sized particles from fig. 6 by Augereau & Beust (2006) based on images in the optical and near-IR. That for  $\beta$  Pic is taken from Fig. 6 by Pantin et al. (1997) based on mid-IR spectra. That for Fomalhaut is from table 1 by Marsh et al. (2005) predicted for a reference wavelength of  $24 \mu\text{m}$  based on  $350, 160$  and  $70 \mu\text{m}$  imaging. (7) The radius of objects initiating the collisional cascade,  $a_{\text{top}}$  is estimated using equation (16). (8) The surface density  $\Sigma(a_{\text{top}})$  is estimated using equation (17). (9) The product of the surface density times the mass ( $\Sigma m(a_{\text{top}})$ ) is estimated for bodies initiating the collisional cascade. (10) The product of the surface density times the mass is estimated using equation (18) for bodies responsible for thickening the disc. Computed quantities listed in Rows 7–10 have been done with parameter  $f_\tau = 4$  (defined in equation 15).

$\bar{i} = \sqrt{\langle i^2 \rangle}$  and  $\langle i^2 \rangle$  is the inclination dispersion. Subsequently, we also refer to  $\bar{e} = \sqrt{\langle e^2 \rangle}$  where  $\langle e^2 \rangle$  is the eccentricity dispersion. We assume a Rayleigh distribution of particle inclinations and eccentricities.

We review how the dust opacity and the disc thickness can be used to estimate the planetesimal size distribution. Dust production in a destructive collisional cascade can in its simplest form be studied with a power-law size distribution. The single power-law form for the size distribution is in part based on the simplest assumption that the specific energy (kinetic energy per unit mass),  $Q_d^*$ , required to catastrophically disrupt a body is a fixed number independent of body radius (often  $2 \times 10^6 \text{ erg g}^{-1}$  for icy bodies are used based on the estimates by Kenyon & Luu 1999). The number of particles with radius  $a$  in a logarithmic bin of size  $d \ln a$  is predicted to be

$$\frac{dN}{d \ln a} \equiv N(a) \propto a^{1-q}. \quad (1)$$

Using a logarithmic bin gives the same scaling with  $a$  as a cumulative distribution  $N_{>a}$  (see appendix A in O'Brien & Greenberg 2005). In an infinite destructive self-similar collisional cascade, the exponent is predicted to be  $q = 3.5$  (Dohnanyi 1968; Tanaka, Inaba & Nakazawa 1996; Davis & Farinella 1997; Kenyon 2002). The main asteroid belt, if fit with a single power law, has a lower exponent of  $q \sim 2.3$  (Ivezic et al. 2001). It is collisionally evolved but deviates from  $q = 3.5$  because of additional removal mechanisms (e.g. Yarkovsky drift and resonances) and because the material properties depend non-trivially on size (O'Brien & Greenberg 2005). In

contrast, the larger bodies in the Kuiper belt are consistent with  $q \sim 5$  (Bernstein et al. 2004). Because of their low number, these do not collide often enough to be part of an ongoing destructive collisional cascade. The high exponent probably reflects conditions during the early Solar system when planetesimals were growing as well as colliding (e.g. Wetherill & Stewart 1993; Kokubo & Ida 1996).

The number of objects of radius  $a$  can be estimated from another of radius  $a_d$  using the scaling relation:

$$N(a) = N_d \left( \frac{a}{a_d} \right)^{1-q}. \quad (2)$$

This relates the number of larger particles to the smallest and so observable particles. Estimates of the number of dust particles,  $N_d$ , as a function of their radius,  $a_d$ , can be made from studies of optical, infrared (IR) and submm observations. It must be kept in mind that because of the uncertainty in the exponent  $q$ , it is difficult to be accurate when extrapolating over orders of magnitude in the size distribution (e.g. Thebault, Augereau & Beust 2003; Krivov, Lohne & Sremcevic 2006; Thebault & Augereau 2007).

The fractional area covered by particles of radius  $a$  or  $\tau(a)$  in a log radial bin can be similarly estimated. Because the opacity depends on the number per unit area times the cross-section area, our assumed power law gives for the opacity integrated over a log radial bin

$$\tau(a) = \frac{d\tau}{d \ln a} = \tau_d \left( \frac{a}{a_d} \right)^{3-q}, \quad (3)$$

where  $\tau_d = \pi a_d^2 s(a_d)$  and  $s(a_d)$  is the number of particles per unit area with radius  $a_d$  in a log radial bin. Likewise, the surface mass density:

$$\Sigma(a) = \Sigma_d \left( \frac{a}{a_d} \right)^{4-q}, \quad (4)$$

where  $\Sigma_d \approx \tau_d \rho_d a_d$ . For  $q = 3.5$ , most of the disc mass is in the largest particles or at the top of the cascade. Gravitational stirring and dynamical friction heating and cooling rates are proportional to the product of the surface density times the mass (e.g. equations 6.1 and 6.2 in Stewart & Ida 2000), scaling as

$$\Sigma(a)m(a) = \Sigma_d m_d \left( \frac{a}{a_d} \right)^{7-q}, \quad (5)$$

where  $\Sigma_d m_d \approx \tau_d \rho_d^2 a_d^4$ . Even when the size distribution is as steep as that for the large objects in the Kuiper belt ( $q \sim 5$ ) gravitational stirring is dominated by the largest bodies.

The optical depth is related to the collision time. For a population of identical objects the collision time-scale

$$t_{\text{col}} \sim (3\tau\Omega)^{-1} \quad (6)$$

(Hanninen & Salo 1992), where  $\Omega$  is the mean motion (angular rotation rate for a particle in a circular orbit) at radius  $r$ . Since the collision lifetime is proportional to the inverse of the optical depth, the time-scale for a particle of radius  $a$  to hit another with the same size scale (again in log radial bins) is

$$t_{\text{col},s}(a) \approx t_{\text{col},d} \left( \frac{a}{a_d} \right)^{q-3}. \quad (7)$$

As explored by Dominik & Decin (2003) and Wyatt et al. (2007), smaller particles are capable of dispersing a larger one if the specific energy of the collision exceeds the critical value. The collision lifetime is shorter by a factor of  $\approx \epsilon^{1-q}$  (equations 21 and 22, and

associated discussion by Dominik & Decin 2003), where  $\epsilon^{-1}a$  is the radius of a smaller particle capable of disrupting one with radius  $a$ . The parameter  $\epsilon$  is estimated by considering what energy projectile object can disrupt the target,

$$\epsilon \sim \left[ \frac{v_{\text{rel}}^2}{2Q_{\text{D}}^*(a)} \right]^{1/3} \quad (8)$$

(approximating equation 25 by Dominik & Decin 2003),<sup>1</sup> where  $v_{\text{rel}}^2$  is the relative or interparticle velocity dispersion. We expect the relative velocity dispersion is twice the particle velocity dispersion or  $v_{\text{rel}}^2 \sim 2u^2$ .

We can now estimate the collisional lifetime for particles in a log radial bin taking into account collisions with smaller particles. After multiplying by equation (8), equation (7) becomes

$$\frac{t_{\text{col}}(a)}{t_{\text{col,d}}} \approx \left( \frac{a}{a_{\text{d}}} \right)^{q-3} \left( \frac{u^2}{Q_{\text{D}}^*} \right)^{(1-q)/3} \quad (9)$$

For  $q = 3.5$ , the time-scale  $t_{\text{col}}(a) \propto a^{0.5}$  is consistent with equation (23) by Dominik & Decin (2003). The maximum radius object that will disrupt during the lifetime of the system is found by setting  $t_{\text{col}}(a)$  to the age of the system,  $t_{\text{age}}$ , and solving equation (9) for  $a$ . This estimate was also used by Wyatt & Dent (2002) in their section 5.3. In other words, we define a radius,  $a_{\text{top}}$ , such that  $t_{\text{col}}(a_{\text{top}}) = t_{\text{age}}$  or

$$a_{\text{top}} = a_{\text{d}} \left( \frac{u^2}{Q_{\text{D}}^*} \right)^{(q-1)/(3(q-3))} (t_{\text{age}} 3\tau_{\text{d}} \Omega)^{1/(q-3)} \quad (10)$$

For  $q = 3.5$ , this gives

$$a_{\text{top}} = a_{\text{d}} \left( \frac{u^2}{Q_{\text{D}}^*} \right)^{5/3} \left( \frac{t_{\text{age}}}{P} \right)^2 (6\pi\tau_{\text{d}})^2, \quad (11)$$

where  $P$  is the rotation period at radius  $r$ . If the disc is hotter or older, then a higher surface density disc that contains more massive bodies is required to initiate the collisional cascade and account for the dust production.

Objects of radius  $a_{\text{top}}$  are those likely to be currently initiating the collisional cascade. Using equation (4) with  $a_{\text{top}}$ , we can estimate the total surface density in these massive objects. As the disc grinds up and is depleted, more massive but lower number density objects can enter and generate the cascade.

## 2.1 In relation to observables

We first relate the disc aspect ratio,  $h$ , to the velocity dispersion and the inclination and eccentricity dispersions. A population of low-inclination orbits has  $\langle z^2 \rangle \approx \frac{r^2 \langle i^2 \rangle}{2}$ , so  $\bar{i} \sim \sqrt{2}h$ . An isotropically scattering disc is expected to have  $\bar{i} \sim \bar{e}/2$  (e.g. Inaba et al. 2001). At low eccentricity, the radial velocity dispersion is  $\langle v_r^2 \rangle \sim \langle e^2 \rangle v_K^2/2$ , and the tangential and vertical velocity dispersions are  $\langle v_\phi^2 \rangle \sim \langle v_z^2 \rangle \sim \langle e^2 \rangle v_K^2/8$ , where  $v_K$  is the velocity of a particle in a circular orbit (e.g. see equations C10a,b by Wetherill & Stewart 1993). The total velocity dispersion is the sum of the three velocity components corresponding to  $u^2 \sim \frac{3}{4} \langle e^2 \rangle v_K^2$  or

$$u \sim \sqrt{3} \bar{i} v_K \sim \sqrt{6} h v_K. \quad (12)$$

These approximations are consistent with  $v_{\text{rel}}^2 = (1.25\bar{e}^2 + \bar{i}^2)v_K^2$

<sup>1</sup> The square root term in equation (25) by Dominik & Decin (2003) should be positive.

used by previous studies (Wetherill & Stewart 1993; Wyatt & Dent 2002).

In equation (3), we described the scaling of opacity in a log radial bin. The normal disc opacity inferred from observations at wavelength  $\lambda$  depends on the disc emissivity or absorption coefficient (here, denoted by  $Q$ )

$$\bar{\tau}(\lambda) \approx \int_{a_{\text{min}}}^{a_{\text{max}}} \frac{\tau(a)}{a} Q(\lambda, a) da. \quad (13)$$

This is consistent with our definition for  $\tau(a)$  (equation 3) and approximations commonly used in interpreting observed fluxes [e.g. equation 1 in (Backman, Witteborn & Gillett 1992) relating dust opacity to flux and the definition given in the caption of fig. 6 in (Pantin, Lagage & Artymowicz 1997)]. The simplest models for the absorption or emissivity coefficient of a particle estimate that these coefficients are

$$Q(\lambda, a) \approx \begin{cases} 1 & \text{for } \lambda \leq a \\ \left( \frac{\lambda}{a} \right)^{-n} & \text{for } \lambda > a \end{cases} \quad (14)$$

(e.g. Backman et al. 1992; Wyatt & Dent 2002) with  $n \sim 1$ . For  $n \sim 1$  and  $q \sim -3.5$  by integrating equation (13), we find that  $\bar{\tau}(\lambda) \sim 4\tau(a = \lambda)$ .

More detailed modelling of the absorption coefficients (e.g. Pollack et al. 1994) shows deviations from this simplest model with strong structure at specific wavelengths such as the 10  $\mu\text{m}$  silicate feature. In addition, the exponent  $q$  describing the dust size distribution, may not be well-constrained, may not be the same for small dust particles as for larger ones or the size distribution may deviate from a power-law form (e.g. Thebault et al. 2003; Augereau & Beust 2006; Krivov et al. 2006; Thebault & Augereau 2007). The wavelength at which the absorption coefficient begins to drop for equation (14) may depend on dust composition (see discussion in appendix D by Backman et al. 1992). Multiwavelength observations are required to better model the size distribution and composition of the dust. To take this uncertainty into account, we describe our estimates in terms of a factor  $f_\tau$ , such that

$$\tau(a = \lambda) = \frac{\bar{\tau}(\lambda)}{f_\tau} \quad (15)$$

that relates the opacity estimated at a wavelength based on observations to the size distribution of particles with radius equal to that wavelength.

An estimate of normal disc opacity at a particular radius requires modelling the surface brightness distribution (Krist et al. 2005; Augereau & Beust 2006; Golimowski et al. 2006). Unfortunately, normal disc opacity estimates are available only at a few wavelengths for the three discs, we are considering here and not all of these are based on multiwavelength models. While optical and near-IR wavelength observations tend to better resolve the discs, they may not accurately predict the mm size distribution (e.g. see the discussion comparing the optical and near-IR opacities to that predicted from the submm for AU Mic by Augereau & Beust 2006). We summarize the existing observed optical depth measurements for these three discs in Table 1 and in the associated table notes, but note that there is uncertainty in the conversion factor  $f_\tau$  between the measured optical depths and the opacity function that we have use here,  $\tau(a_{\text{d}})$ , the optical depth integrated in a log radial bin of size 1 for dust particles of size  $a_{\text{d}} = \lambda$ . As the opacity of smaller grains is sensitive to the removal process as well as collisions, it is important to use observed opacity that is dominated by particles that are not affected by radiative forces (e.g. see discussion by Dominik & Decin 2003).

We now convert equation (11) into a form more easily computed from observables. The observables are the disc aspect ratio,  $h$  and the normal disc opacity  $\bar{\tau}(\lambda)$  at wavelength  $\lambda$ . The size of the objects initiating the collisional cascade when  $q = 3.5$

$$a_{\text{top}} \approx 5.4 \text{ km} \left( \frac{\lambda}{10 \mu\text{m}} \right) \left( \frac{M_*}{M_\odot} \right)^{8/3} \left( \frac{r}{100 \text{ au}} \right)^{-14/3} \\ \times \left( \frac{Q_D^*}{2 \times 10^6 \text{ erg g}^{-1}} \right)^{-5/3} \left( \frac{t_{\text{age}}}{10^7 \text{ yr}} \right)^2 \left( \frac{h}{0.02} \right)^{10/3} \\ \times \left[ \frac{\bar{\tau}(\lambda)}{10^{-2}} \right]^2 \left( \frac{f_\tau}{4} \right)^{-2}. \quad (16)$$

Because we have scaled with the inclination or aspect ratio instead of the collision velocity, the exponent of  $r$  and  $M_*$  differ from but are consistent with equation (36) by Dominik & Decin (2003). The relation also differs from previous work (Wyatt & Dent 2002; Dominik & Decin 2003; Wyatt et al. 2007) because we have based our estimate on a collision time-scaled from the face on disc opacity at a particular radius rather than the total fraction of starlight re-emitted in the IR.

Inserting our value for the  $a_{\text{top}}$  into equation (4) yields an estimate for the total disc density,

$$\Sigma(a_{\text{top}}) \approx 0.0018 \text{ g cm}^{-2} \left( \frac{\rho_d}{1 \text{ g cm}^{-3}} \right) \left( \frac{M_*}{M_\odot} \right)^{4/3} \left( \frac{r}{100 \text{ au}} \right)^{-7/3} \\ \times \left( \frac{Q_D^*}{2 \times 10^6 \text{ erg g}^{-1}} \right)^{-5/6} \left( \frac{t_{\text{age}}}{10^7 \text{ yr}} \right) \left( \frac{h}{0.02} \right)^{5/3} \\ \times \left( \frac{\lambda}{10 \mu\text{m}} \right) \left[ \frac{\bar{\tau}(\lambda)}{10^{-2}} \right]^2 \left( \frac{f_\tau}{4} \right)^{-2}. \quad (17)$$

We have assumed here that the collision cascade started very early in the life of the system; however, at early stages the interparticle velocities were probably not high enough for destructive collisions (Kenyon & Bromley 2001; Dominik & Decin 2003). If the time-scale of the destructive cascade were smaller than  $a_{\text{top}}$  and  $\Sigma(a_{\text{top}})$  would both be smaller than the estimates given above.

The product of the density times the mass for the bodies initiating the cascade  $a_{\text{top}}$

$$(\Sigma m)(a_{\text{top}}) \approx 8.9 \times 10^{15} \text{ g}^2 \text{ cm}^{-2} \\ \times \left( \frac{M_*}{M_\odot} \right)^{28/3} \left( \frac{r}{100 \text{ au}} \right)^{-49/3} \\ \times \left( \frac{Q_D^*}{2 \times 10^6 \text{ erg g}^{-1}} \right)^{-35/6} \left( \frac{t_{\text{age}}}{10^7 \text{ yr}} \right)^{7/2} \\ \times \left( \frac{\lambda}{10 \mu\text{m}} \right)^4 \left( \frac{\tau_d}{10^{-3}} \right)^8 \left( \frac{f_\tau}{4} \right)^{-8} \\ \times \left( \frac{h}{0.02} \right)^{35/3} \left( \frac{\rho_d}{1 \text{ g cm}^{-3}} \right)^2. \quad (18)$$

### 3 HEATING THE DISC WITH GRAVITATIONAL STIRRING

We explore the idea that the observed thickness of the disc is due to gravitational stirring by bodies of mass,  $m_s$ , surface density,  $\Sigma_s$ , and size  $a_s$ . We define a mass ratio  $\mu_s \equiv \frac{m_s}{M_*}$  and surface density ratio

$\sigma_s \equiv \frac{\Sigma_s r^2}{M_*}$ . If the disc is in collisional equilibrium then we expect that  $\bar{e} \sim 2\bar{i}$ .

In the dispersion-dominated regime, and assuming that the dispersions of the tracer particles exceed those of the massive particles doing the stirring ( $\bar{i} > \bar{i}_s$  and  $\bar{e} > \bar{e}_s$ ),

$$\frac{1}{\Omega} \frac{d(i^2)}{dt} \approx \frac{\sigma_s \mu_s B J_z(\beta) \beta}{\sqrt{\pi} (i^2)} \quad (19)$$

(based on equation 6.2 by Stewart & Ida 2000) where  $\beta = \frac{\bar{i}}{\bar{i}_s} \sim 0.5$  (corresponding to equation 2.11 by Stewart & Ida 2000). The function described by Stewart & Ida (2000)  $J_z(\beta = 0.5) \approx 2.0$ . The coefficient  $B \sim 2 \ln \Lambda$  and we estimate  $\Lambda$  using equation 2.7 by Stewart & Ida (2000)

$$\Lambda \approx 3\mu_s^{-1} \bar{i}^3. \quad (20)$$

As the coefficient,  $B$ , only depends logarithmically on  $\Lambda$ , we can use the scaleheight estimated from observations to estimate  $\Lambda$  and we can solve equation (19) finding that  $\bar{i} \propto t^{-1/4}$ , specifically

$$\bar{i}(t) \approx \left( \frac{2 \ln \Lambda \Omega t \sigma_s \mu_s}{\sqrt{\pi}} \right)^{1/4}. \quad (21)$$

The above equation can be inverted at time  $t_{\text{age}}$

$$\sigma_s \mu_s \approx \frac{\bar{i}^4 P}{4 \ln \Lambda \sqrt{\pi} t_{\text{age}}}, \quad (22)$$

where we have set  $P$  to be the rotation period at  $r$ .

In terms of observables, this leads to a constraint on the largest bodies with size  $a_s$

$$(\Sigma m)(a_s) \approx 2.4 \times 10^{24} \text{ g}^2 \text{ cm}^{-2} \left( \frac{h}{0.02} \right)^4 \left( \frac{t_{\text{age}}}{10^7 \text{ yr}} \right)^{-1} \\ \times \left( \frac{M_*}{M_\odot} \right)^{3/2} \left( \frac{r}{100 \text{ au}} \right)^{-1/2} \left( \frac{\ln \Lambda}{12} \right)^{-1}. \quad (23)$$

We note that the constraint on the product of the surface density times the mass of the largest bodies is independent of the disc opacity. In contrast, the estimates for the top of the collisional cascade (size of object and density) are sensitive to the dust opacity.

### 3.1 Connecting the size distributions

Equation (16) gives us an estimate for the size of the bodies at the top of the collisional cascade, and equation (18) gives us the surface density times mass in the disc for these bodies. This product is well below that needed to account for the disc thickness with gravitational stirring (equation 23). To find the size,  $a_s$ , of the bodies responsible for the gravitational stirring, we must extend the size distribution beyond  $a_{\text{top}}$ .

Unfortunately, for bodies with sizes  $a > a_{\text{top}}$ , we can no longer assume a size distribution consistent with a collisional cascade. There are few guidelines on what type of power law to use for bodies greater than 10 km. The only known system that differs significantly from the size distribution expected from collisional evolution might be the largest bodies in the Kuiper belt that have size distribution with power law  $q \sim 5$  (Bernstein et al. 2004). A variety of size distributions might be produced during the phase of planetesimal growth with low values for the exponent  $q$  at the high-mass end implying runaway growth (e.g. Wetherill & Stewart 1993; Kokubo & Ida 1996; Inaba et al. 2001).

To place constraints on the size and density of the largest bodies and exponent of the size distribution for these bodies, we compare

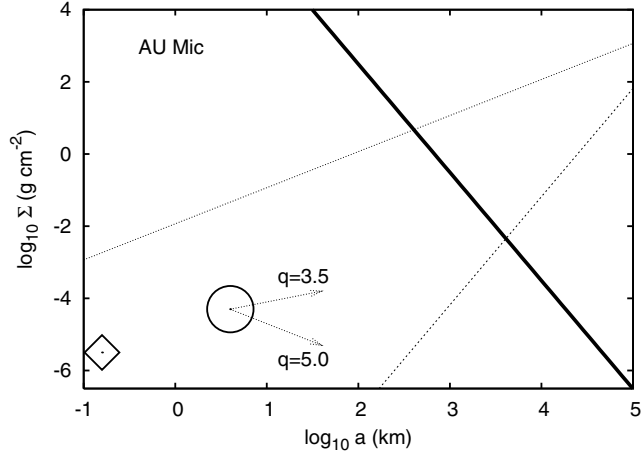


**Figure 1.** The thick solid line shows the constraint on the product of the surface density times mass in the most massive bodies present for AU Mic, required to account for the disc thickness from heating by gravitational stirring. This is computed using equation (23) and values listed in Table 1. The upper dotted line shows the upper limit on the surface densities for these massive bodies set by requiring that they be on averaged spaced further apart than their mutual Hill spheres (equation 24). The lower dotted line shows the lower limit on their surface density set by requiring more than a few bodies of this mass reside in the disc (equation 25). The large circle is placed at the estimated location of the top of the collisional cascade (computed using equations 16 and 18 and listed in Table 1). Arrows are shown with slopes predicted for size distributions with  $q = 3.5$  and  $5$ . The size distribution must connect the circle and the segment of the thick solid line that lies between the two dotted thin lines. The large circle was estimated using a size distribution with  $q = 3.5$ . For  $q = 3.6$ , the estimated top of the collisional cascade would be at the location of the diamond.

our constraint on the product of the surface density and mass of the largest bodies to the surface density and size of the bodies initiating the collisional cascade.

In Fig. 1, we plot the constraint on the product of disc surface density times mass for AU Mic. This constraint corresponds to a surface density as a function of the radius of a body and is computed from equation (23) using values listed in Table 1 and  $f_\tau = 4$ . The horizontal axis is log radius instead of log mass, so the slope of this constraint is  $-3$ . The conversion between mass and radius has been done with a density of  $1 \text{ g cm}^{-3}$ . On this plot, we have plotted as dotted lines two other constraints on bodies in the disc. We estimate that the most massive bodies cannot on average be closer together than their mutual Hill spheres,

$$\Sigma(m) \lesssim \frac{m}{r_{\text{mH}}^2}, \quad (24)$$

where the mutual Hill radius for two bodies of similar mass  $r_{\text{mH}} \equiv r(\frac{2m}{3M_*})^{1/3}$ . This constraint gives the upper dotted line. We also require that the number of bodies should not be extremely low,

$$\Sigma(m) \gtrsim \frac{10m}{\pi r^2}. \quad (25)$$

This constraint is plotted as the lower dotted line. The range of densities for the most massive bodies in the disc must lie on the solid one and between the two dotted ones. Also plotted on this plot is the estimated density,  $\Sigma(a_{\text{top}})$ , and radius,  $a_{\text{top}}$ , of the particles initiating the cascade. Arrows are drawn for surface densities  $\Sigma(a)$  that have size distributions with exponents  $q = 3.5$  and  $5.0$  and that have  $\Sigma(a_{\text{top}})$ . The circle showing the top of the collisional cascade must be connected to the thick solid line segment that lies between

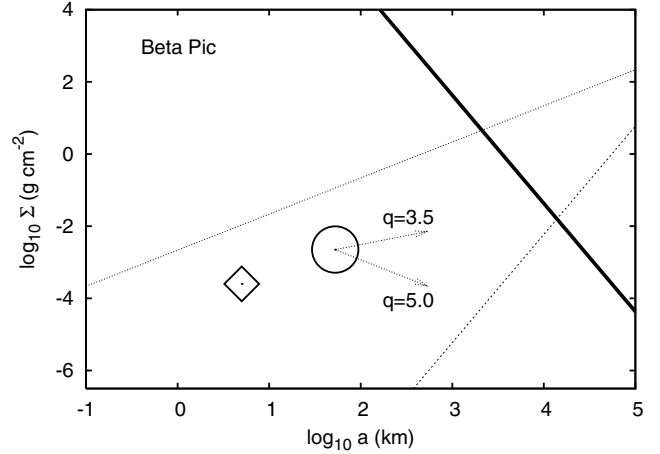


**Figure 2.** Similar to Fig. 1 except for  $\beta$  Pic's disc.

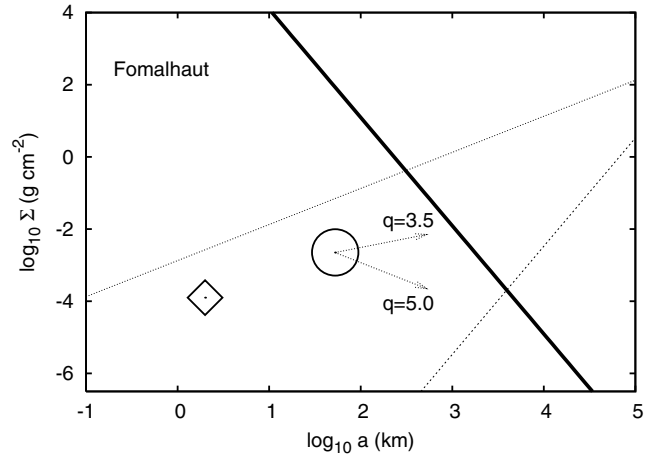


**Figure 3.** Similar to Fig. 1 except for Fomalhaut's disc.

the two dotted ones to estimate the exponent of the size distribution for  $a > a_{\text{top}}$ .

The solid thick line segment between the two thin dotted lines in Fig. 1 suggests that 1000 km bodies reside in AU Mic's disc even though the collisional cascade only requires bodies of radius a few km. We have checked that our estimated value of 12 for  $\log \Lambda$  is consistent with the mass of these 1000 km bodies and the disc thicknesses (equation 20). For  $q > 4$ , most of the disc mass resides in the most massive bodies. Connecting the circle with the line segment requires a slope shallower than  $q = 3.0$ . Most of the disc mass must reside in 1000 km embryos in AU Mic's disc to account for its thickness even though only km-sized bodies are required to account for its dust production.

Figs 2 and 3 are similar to Fig. 1 except computed for  $\beta$  Pic's and Fomalhaut's discs also using parameters listed in Table 1. We attribute the differences in these figures primarily to the observed thickness as  $a_{\text{top}} \propto h^{10/3}$  (equation 16).  $\beta$  Pic's disc is quite a bit thicker than Fomalhaut's or AU Mic's so its collisional cascade is more efficient and so requires higher mass progenitors. Fomalhaut is older allowing a lower density disc to account for the thickness.

Gravitational stirring requires similar-sized embryos for the three discs but for Fomalhaut the mass and surface density of the bodies is only an order of magnitude larger than that predicted from estimating the top of the collisional cascade. Nevertheless, the bodies we infer

at the top of the collisional cascade are not sufficiently dense and massive to account for the thickness of this disc.

A comparison between the surface densities in the bodies required to account for the disc thickness and that predicted at the top of the collision cascade allows exponents  $q \lesssim 3, 3.5$  and  $4.5$  for the three discs, AU Mic,  $\beta$  Pic and Fomalhaut, respectively. The extremely shallow exponent for AU Mic at the top end suggests that the size distribution deviates from power-law form. A curve in the size distribution at the high-mass end has been predicted by models and simulations of planetesimal accretion when the disc contains embryos in a stage of runaway growth (Wetherill & Stewart 1993; Kokubo & Ida 1996; Inaba et al. 2001).

We have only considered the effect of gravitational stirring in the dispersion-dominated regime. Now that we have an estimate for the masses of the most massive bodies residing in these discs, we check this assumption. Only for  $a > 1.2 \times 10^4$  km does a body's Hill radius approach a scaleheight  $r\bar{i}$  for an inclination  $\bar{i} = 0.01$ . The dispersion-dominated gravitational stirring estimate used in equation (19) (rather than a sheer dominated one) is therefore reasonable. Previous work has found that passage through the sheer-dominated regime is comparatively fast (e.g. Kenyon & Bromley 2001). A better estimate would take into account both regimes, though the improved constraints on the massive bodies should not significantly deviate from those estimated here.

The largest uncertainty in our estimates is due to uncertainty in the power-law exponent  $q$  since we have extrapolated over about 10 orders of magnitude in the size distribution. In Figs 1–3, we also plot as diamonds  $a_{\text{top}}$  and  $\Sigma(a_{\text{top}})$  estimated for an exponent  $q = 3.6$  that is 0.1 larger than assumed previously using equation (10). This estimate is not self-consistent as only a change in the collisional statistics (e.g. that would be caused by a size-dependent change in  $Q_D^*$ ) would change the size distribution. Nevertheless, this procedure should allow us to estimate how our value for  $a_{\text{top}}$  and  $\Sigma(a_{\text{top}})$  depends on  $q$ .

An increase in  $q$  causes a decrease in both the estimated size,  $a_{\text{top}}$  (equation 10) and surface density,  $\Sigma(a_{\text{top}})$  (equation 4). Thus, variations in  $q$  cause the estimated point corresponding to the top of the cascade to move along a line that is nearly parallel to the upper dotted lines shown in the figures. Uncertainty in  $q$  only affects our estimate of the size and mass density of objects likely to initiate the collisional cascade (equation 10) and not those of objects responsible for gravitational stirring (equation 23). If the exponent is higher than  $q = 3.5$  then the comparison between the top of the cascade and the mass surface density required to account for the disc thickness yields similar but stronger results to those discussed previously. All three discs would require a low exponent,  $q \lesssim 3.5$ , in the largest bodies.

If  $q$  in the cascade is lower than 3.5, the estimated size and mass surface density of objects initiating the collision cascade are higher. This moves the top of the cascade to a point that is higher and to the right-hand side of the circles shown in Figs 1–3. As we found before, Fomalhaut's estimated top of the cascade contains nearly enough mass to account for the disc thickness. It is unlikely that  $q \lesssim 3.4$  for Fomalhaut or  $q \lesssim 3.3$  for  $\beta$  Pic and AU Mic otherwise bodies initiating the cascade would have produced a disc thicker than observed. For  $\beta$  Pic and AU Mic, a value of  $q \sim 3.3$  would imply that 1000 km-sized bodies could both initiate the collisional cascade and account for the disc thickness.

#### 4 DISCUSSION

We have used estimates of collisional cascades (e.g. Kenyon 2002; Dominik & Decin 2003; Wyatt et al. 2007) to estimate the size and

surface density of the bodies responsible for initiating the collisional cascade. We have done this for three debris discs, that of AU Mic,  $\beta$  Pic and Fomalhaut, with resolved vertical structure estimating that these bodies have radii of 4, 180 and 70 km, respectively. We have estimated these at the radius at which the surface brightness profile changes slope (also called the break radius). The body sizes are a few times larger than previous estimates (e.g. Wyatt & Dent 2002). The differences arise because we have based our estimate on a collision time-scaled from the face on disc opacity at a particular radius rather than the total fraction of starlight re-emitted in the IR and we have used the observed disc aspect ratio to estimate the velocity of collisions.

Assuming that the smallest particles are heated solely by gravitational stirring from the largest ones, the disc thickness can be used to place a constraint on the product of the surface density times mass of the largest bodies (equation 18). From this we infer that 1000 km radius bodies or planetary embryos are likely to reside in these three discs. The large body sizes do not conflict with the lack of observed gaps in the discs (Quillen 2006, 2007) except possibly for the extreme high-mass end allowed for  $\beta$  Pic's disc. A comparison between the surface densities in these bodies and that predicted at the top of the collision cascade allows exponents  $q \lesssim 3, 3.5, 4.5$  for the three discs AU Mic,  $\beta$  Pic and Fomalhaut, respectively. The shallow exponent for AU Mic at the top end suggests that this disc contains embryos in a stage of runaway growth as predicted by simulations (Wetherill & Stewart 1993; Kokubo & Ida 1996; Inaba et al. 2001). For all three discs, we infer that most of the disc mass is likely to reside in embryos and estimate that the surface densities are of the order of  $10^{-2}$  g cm $^{-2}$ . The largest uncertainty in our estimate of the size and mass surface density of bodies initiating the collisional cascade arise from the uncertainty of the exponent  $q$  describing the size distribution. If  $q \gtrsim 3.5$  for bodies in the cascade then shallow exponents ( $q \lesssim 3.5$ ) are required for the more massive bodies responsible for gravitational stirring. The exponent of bodies in the cascade must be  $q \gtrsim 3.3$  otherwise they would have caused the disc to be thicker than observed. For Fomalhaut if  $q \sim 3.3$  then the bodies initiating the collisional cascade are sufficiently massive to account for the thickness of the disc.

A number of simplifying assumptions went into estimating the properties of the top of the cascade. We assumed only a single power-law form for the size distribution; however, the specific energy for dispersion is predicted to depend on body size (Benz & Asphaug 1999) so a single power law is not a good assumption (e.g. Krivov et al. 2006; Thebault & Augereau 2007). The discs may not have been sufficiently excited for efficient dust production during the entire lifetime of these systems (Dominik & Decin 2003). A shorter collisional lifetime would lead to a lower surface density and size estimated for the top of the cascade (see equations 17 and 16), though taking into account the dependence of the specific energy on size in the regime where self-gravity is important would increase the surface density of larger bodies and might decrease the size at the top of the cascade. The sizes at the top of the cascade predicted here are nearing the threshold for a destructive equal-mass collision at a velocity estimated from the disc thickness, particularly, in the case of Fomalhaut that has a very thin disc but has a large estimated  $a_{\text{top}}$ .

Our estimate of the gravitational stirring rate neglected the role of dynamical friction from smaller particles and the sheer-dominated regime. Both should be taken into account to improve the estimate of size and number of the largest bodies residing in these discs.

Better modelling of the dust distribution using multiwavelength observations and high angular resolution imaging would

significantly improve constraints on the small radius end of the size distribution. While we have found normal disc opacity measurements in a few wavelengths in the literature, the different wavelength estimates, different assumptions for the assumed size distributions and different procedures for modelling the data make it difficult to constrain and compare the dust size distributions and normal disc opacities among the discs.

We have discussed ways to improve the estimates introduced here. We now discuss possible implications based on these predictions. If the size distributions inferred here are common then longer lifetimes would be predicted for dust production because the larger bodies (inferred here), entering the cascade later, contain a reservoir of mass available for dust production at later times. The distribution of disc properties as a function of age can be used to place constraints on planetesimal growth models as well as dust production.

We have only considered opacities at particular radii for these discs. For AU Mic and  $\beta$  Pic, we chose radii at which there is a break (or change in slope) in the surface brightness profile. If the disc aspect ratios do not strongly vary with radius then equation (23) implies that the product of the mass times the surface density in the largest bodies,  $\Sigma m(a_s) \propto r^{-1/2}$  is only weakly decaying with radius. Compare this to  $\Sigma(a_{\text{top}}) \propto \tau_d^{-2} r^{-7/3}$  and  $a_{\text{top}} \propto \tau_d^{-2} r^{-14/3}$  predicted via equations (16) and (17). Both  $\Sigma(a_{\text{top}})$  and  $a_{\text{top}}$  must drop rapidly with radius. If discs are not extremely thin at larger radii then either there is another source of heating at large radii accounting for the disc thickness, or dust particles detected at large radii originate from inner radii and are either blown out or are on highly eccentric orbits (Augereau & Beust 2006; Strubbe & Chiang 2006). A thin and sparse disc will not efficiently produce dust as the collisions are not destructive. Consequently, multiwavelength observations resolving discs as a function of radius should be able to test the utility of the estimates explored here as well as better probe planetesimal growth and evolution with radius.

## ACKNOWLEDGMENTS

We thank the Observatoire de la Côte D'Azur for support, a warm welcome and hospitality during 2007 January. We thank Philippe Thebault, Patrick Michel, Derek Richardson and Hal Levison for interesting discussions and correspondence. Support for this work was in part provided by National Science Foundation grants AST-0406823 & PHY-0552695, the National Aeronautics and Space Administration under Grant No. NNG04GM12G issued through the Origins of Solar Systems Program and HST-AR-10972 to the Space Telescope Science Institute.

## REFERENCES

Augereau J.-C., Beust H., 2006, *A&A*, 455, 987  
 Augereau J.-C., Nelson R. P., Lagrange A. M., Papaloizou J. C. B., Mouillet D., 2001, *A&A*, 370, 447

Backman D. E., Witteborn F. C., Gillett F. C., 1992, *ApJ*, 385, 670  
 Barrado y Navascues D., 1998, *A&A*, 339, 831  
 Barrado y Navascues D., Stauffer J. R., Song I., Caillault J.-P., 1999, *ApJ*, 520, L123  
 Benz W., Asphaug E., 1999, *Icarus*, 142, 5  
 Bernstein G. M., Trilling D. E., Allen R. L., Brown M. E., Holman M., Malhotra R., 2004, *AJ*, 128, 1364  
 Crifo F., Vidal-Madjar A., Lallement R., Ferlet R., Gerbaldi M., 1997, *A&A*, 320, L29  
 Davis D. R., Farinella P., 1997, *Icarus*, 125, 50  
 Dohnanyi J. S., 1968, in Kresak L., Millman P. M., eds, *IAU Symp. 33, Physics and Dynamics of Meteors*. Dordrecht, Reidel, p. 486  
 Dominik C., Decin G., 2003, *ApJ*, 598, 626  
 Golimowski D. A. et al., 2006, *AJ*, 131, 3109  
 Hanninen J., Salo H., 1992, *Icarus*, 97, 228  
 Houdebine E. R., Doyle J. G., 1994, *A&A*, 289, 185  
 Inaba S., Tanaka H., Nakazawa K., Wetherill G. W., Kokubo E., 2001, *Icarus*, 149, 235  
 Ivezić Z. et al., 2001, *AJ*, 122, 2749  
 Kalas P., Graham J. R., Clampin M., 2005, *Nat*, 435, 1067  
 Kenyon S. J., 2002, *PASP*, 114, 265  
 Kenyon S. J., Bromley B. C., 2001, *AJ*, 121, 538  
 Kenyon S. J., Luu J. X., 1999, *AJ*, 118, 1101  
 Kokubo E., Ida S., 1996, *Icarus*, 123, 180  
 Krist J. E. et al., 2005, *AJ*, 129, 1008  
 Krivov A. V., Lohne T., Sremcevic M., 2006, *A&A*, 455, 509  
 Marsh K. A., Velusamy T., Dowell C. D., Grogan K., Beichman C. A., 2005, *ApJ*, 620, L47  
 O'Brien D. P., Greenberg R., 2005, *Icarus*, 178, 179  
 Pantin E., Lagage P. O., Artymowicz P., 1997, *A&A*, 327, 1123  
 Pollack J. B., Hollenbach D., Beckwith S., Simonelli D. P., Roush T., Fong W., 1994, *ApJ*, 421, 615  
 Quillen A. C., 2006, *MNRAS*, 372, L14  
 Quillen A. C., 2007, *MNRAS*, 377, 1287  
 Song I., Caillault J.-P., Barrado y Navascues D., Stauffer J. R., 2001, *ApJ*, 546, 352  
 Stewart G. R., Ida S., 2000, *Icarus*, 143, 28  
 Tanaka H., Inaba S., Nakazawa K., 1996, *Icarus*, 123, 450  
 Thebault P., Augereau J.-C., 2007, *A&A*, in press  
 Strubbe L. E., Chiang E. I., 2006, *ApJ*, 648, 652  
 Thebault P., Augereau J.-C., Beust H., 2003, *A&A*, 408, 775  
 Wetherill G. W., Stewart G. R., 1993, *Icarus*, 106, 190  
 Wyatt M. C., Dent W. R. F., 2002, *MNRAS*, 334, 589  
 Wyatt M. C., Smith R., Greaves J. S., Beichman C. A., Bryden G., Lisse C. M., 2007, *ApJ*, 658, 569  
 Zuckerman B., Song I., Bessell M. S., Webb R. A., 2001, *ApJ*, 562, L87

This paper has been typeset from a  $\text{\TeX}/\text{\LaTeX}$  file prepared by the author.